THESIS FOR THE DEGREE OF LICENTIATE OF ENGINEERING IN SOLID AND STRUCTURAL MECHANICS

Towards a digital twin for prediction of rail damage evolution in railway curves

CAROLINE ANSIN

Department of Industrial and Materials Science
Division of Material and Computational Mechanics
CHALMERS UNIVERSITY OF TECHNOLOGY

Göteborg, Sweden 2023

Towards a digital twin for prediction of rail damage evolution in railway curves
CAROLINE ANSIN

Thesis for the degree of Licentiate of Engineering
Report number: IMS-2023-06

Department of Industrial and Materials Science
Division of Material and Computational Mechanics
Chalmers University of Technology
SE-412 96 Göteborg
Sweden
Telephone: +46 (0)31-772 1000

Cover:
Illustration of digital twin framework, the numerical model is continuously updated by field measurements. In turn, the numerical model can forecast material damage in the rail head. Photo from [1].

Chalmers Reproservice
Göteborg, Sweden 2023

Towards a digital twin for prediction of rail damage evolution in railway curves

CAROLINE ANSIN
Department of Industrial and Materials Science
Division of Material and Computational Mechanics
Chalmers University of Technology

Abstract

Railway maintenance incurs significant expenses, and reducing the costs while maintaining safety levels and functionality is of great industrial and societal interest. Accurately predicting rail damage is crucial for cost-effective maintenance and extending rail life. This thesis focuses on developing a digital twin that can predict the rail damage evolution in a curved track under operational traffic, considering plastic deformation, wear, and surface Rolling Contact Fatigue (RCF) by accurate and fast simulations.

The first part of the thesis contains results from long-term simulations of rail damage for a given traffic scenario. The adopted simulation methodology is calibrated and validated using field tests. The numerical methodology in **Paper A** employs a framework that incorporates multiple steps that are applied iteratively to predict rail head degradation. The different steps are (1) the dynamic vehicle-track interaction for a given load sequence, (2) elastic-plastic wheel-rail contact, (3) accumulative rail damage due to cyclic plasticity, wear, and surface RCF, and (4) rail profile update from the accumulated wear and plasticity. Thereafter, the simulation steps can be repeated. It is demonstrated how the numerical model can be calibrated to match field measurements of the averaged geometry changes of the rail cross-section and predict surface RCF crack initiation. To allow for better predictions of the local wear distribution on the rail head, a model sensitivity study is performed in **Paper B** to determine the most significant model parameters for vehicle and track. Also, the effect of different contact modeling approaches is investigated. By including a freight vehicle, using different measured wheel profile samples in the load sequence, and considering a different contact modeling approach, promising predictions of the wear distribution are obtained.

Furthermore, a reduced-order model based on Proper Generalized Decomposition (PGD) is developed in **Paper C** for accurately simulating the deformation in the rail under varying contact loads. It enables cost-efficient simulations required for the digital twin framework. As a first step towards replacing computationally demanding nonlinear finite element simulations for the plastic deformation evaluation, the current version of the PGD model involves a domain decomposition of a three-dimensional elastic rail head combined with a parameterized discrete load to account for different load scenarios in an automated fashion. It is shown that the three-dimensional PGD model can be computed with two-dimensional complexity and can generate the parametrized displacement field for various loading scenarios.

Keywords: Railway, plasticity, wear, Rolling Contact Fatigue (RCF), Finite Element Modelling (FEM), digital twin, Proper Generalized Decomposition (PGD), model reduction, dynamic vehicle-track interaction

To my parents; Annika and Robert.

Preface

This work was carried out at the Department of Industrial and Materials Science at Chalmers University of Technology between December 2020 and May 2023. The research project MU40 "Digital Twin of Reprofiled Rails" is part of Chalmers Railway Mechanics (CHARMEC). Parts of the study were funded by the European Union's Horizon 2020 research and innovation program under the In2Track2 and In2Track3 projects under grant agreements numbers 826255 and 101012456. The simulations were enabled by resources provided by the Swedish National Infrastructure for Computing (SNIC) at the Chalmers Center for Computational Science and Engineering (C3SE).

Acknowledgements

First and foremost, I would like to extend my appreciation to my supervisors Professor Fredrik Larsson, Professor Magnus Ekh, Associate Professor Björn Pålsson, and Professor Ragnar Larsson for all of the guidance and support you have given me throughout my research project. Working with you always results in fruitful discussions and new insights. I cannot thank you enough for the work we have done together and I look forward to our continued collaboration in this project!

I would also like to acknowledge the CHARMEC research group and all the partners we collaborate with, for your valuable input and interesting discussions during our workshops.

I want to thank all my friends and colleagues for the great work atmosphere, and all the fun times. I appreciate working alongside you!

Lastly, I would also like to express my sincere gratitude to my family and friends for your kind support. And a special thanks to my boyfriend, Love, for your endless patience, support, and encouragement.

Gothenburg, May 2023
Caroline Ansin

Thesis

This thesis consists of an extended summary and the following appended papers:

Paper A C. Ansin, B. Pålsson, M. Ekh, F. Larsson and R. Larsson, "Simulation and field measurements of the long-term rail surface damage due to plasticity, wear and surface rolling contact fatigue cracks in a curve". *Proceedings 12th International Conference on Contact Mechanics and Wear of Rail/Wheel Systems (CM2022)*, Melbourne (Australia) September 2022, 11 pp

Paper B C. Ansin and B. Pålsson. "Influence of model parameters on the rail profile wear distribution in a curve". *Internal report, Chalmers University of Technology, 2023.*

Paper C C. Ansin, F. Larsson and R. Larsson. "Fast Simulation of 3D Elastic Wheel-Rail Contact Using Proper Generalized Decomposition". *Manuscript to be submitted for publication.*

The appended papers were collaboratively prepared with co-authors. The author of this thesis was responsible for a major part of the work and contributed as follows: took part in planning the papers, developed theoretical and computational framework, performed numerical implementations and simulations, and wrote the papers.

Contents

Part I
Extended Summary

CHAPTER 1

Introduction

In this chapter, the research topic is presented along with some of the background and underlying motivation for the work.

1.1 Background and motivation

In curved tracks, high lateral contact forces cause damage to the rails through wear, plasticity, and surface or subsurface Rolling Contact Fatigue (RCF) crack initiation and propagation. This damage can result in train delays or traffic interruptions due to rail failures, frequent physical inspections, grinding, or installation of new rails. In fact, RCF defects were estimated to cost roughly €300 million annually in the European rail system in the year 2000 [2] and have certainly increased since then. Predicting and detecting when rails need maintenance is crucial to optimize timing and type of action, which can improve punctuality and traffic capacity and result in cost reductions. Also, an early repair can prevent damage acceleration and extend rail life [3].

1.2 Damage mechanisms

Damage to rails of curved tracks is influenced by various factors such as the characteristics of traffic loading, the curve radius, wheel and rail profiles, and the type of rail material used. The diversity of traffic situations gives rise to different contact scenarios, with varying load magnitudes and contact positions along the rail profile's cross-section. In curved tracks, a common contact scenario is a two-point contact on the outer rail, as

shown in Figure 1.1, where the wheel flange is pushed towards the gauge corner of the rail. Multiple contacts can also occur due to irregularities in the wheel and rail profiles.

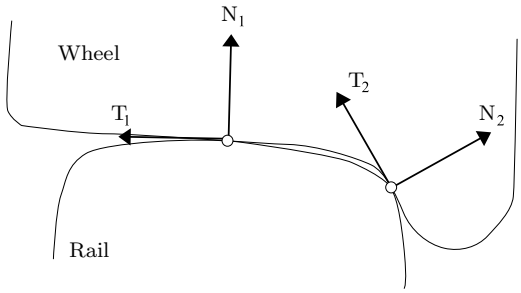

Figure 1.1: *Two-point contact between wheel and rail gives rise to normal N and tangential T loads at each contact.*

When the two bodies are pressed together a small contact area arises for which the magnitude of the contact pressure between wheel and rail can be of the order 1000 to 1500 MPa [4], which may result in damage to both the wheel and rail. Common damage mechanisms observed in rails include wear, plastic deformation, and surface (or subsurface) cracks initiated by RCF, as illustrated in Figure 1.2.

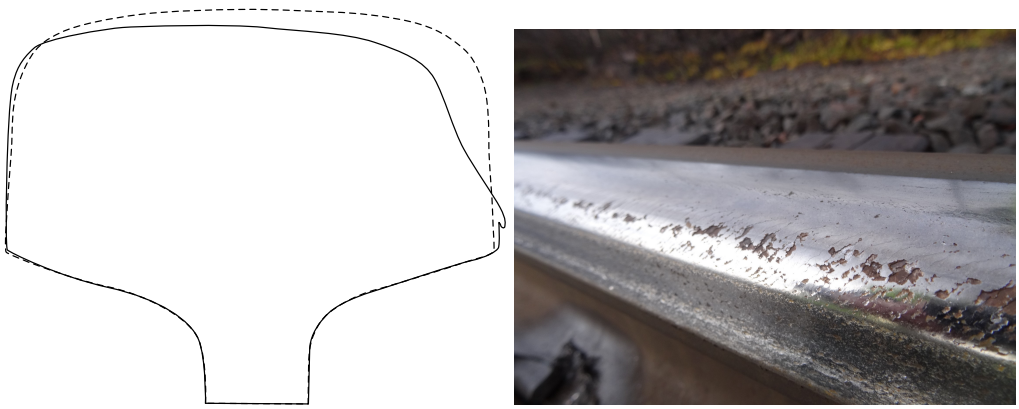

(a) ***(b)***

Figure 1.2: *(a) nominal (BV50) and worn rail profile from [5], and (b) gauge corner RCF cracks. Picture from Anders Ekberg.*

Wear is a common damage mechanism in small radius curves, and it is caused by the gradual loss of material from the contact surface. Wear is influenced by factors such as contact conditions (e.g., sliding velocity and contact pressure), material properties of the contact surface, and the presence of debris [6]. Wear can be classified into different regimes, e.g., mild or severe, and can vary along the profile. In general, wear is more severe at the gauge corner of the rail profile compared to the top, (cf. Figure 1.2a).

According to Olofsson et al. [7], the wear rate at the gauge corner can be up to ten times higher than at the top of the rail.

Plastic deformation can also occur in curves, and plastic flow can lead to the formation of a lip beneath the gauge corner of the outer rail as shown in Figure 1.2a [5, 7]. This redistribution of material is due to the yield limit being exceeded in the material caused by normal and tangential contact traction. In the contact region, cyclic loading causes inelastic deformation to accumulate and residual stresses to develop [8]. Consequently, the material work-hardens and develops texture over time. A work-hardened material has an increased yield strength and hardness, especially near the contact surface, making the properties vary across the profile [9, 10]. Texture development results in an anisotropic surface layer [11], which, as demonstrated by Larijani et al. [12], can control crack propagation in the rail.

The development of cracks due to RCF is a dominant damage mechanism for shallower curves. RCF cracks are closely related to plastic deformation since they are caused by severe shearing of the surface material which leads to fatigue and exhaustion of the ductility of the material (ratcheting) [13]. A work-hardened material, on the other hand, can affect both resistance to cracks growth and wear [8, 10] while wear can remove (or reduce the length of) RCF cracks and hardened material. The crack path can then continue in different directions such as branching toward the surface or propagating downwards. If the crack branches toward the surface it may cause portions of the surface material to detach, called spalling (cf. Figure 1.2b). If the crack propagates downwards it can cause transverse failure and potentially lead to a rail breakage which may cause a derailment.

1.3 Research scope

The ultimate goal of this research is to develop a digital twin that can predict the rail damage evolution under operational traffic in a railway curve. A digital twin is a numerical model of a physical counterpart, in this case, a representative cross-section of the outer rail head, with the goal of simulating and capturing its geometry changes in the field over time, see Figure 1.3. The digital twin is continuously updated with field measurements to validate and improve the simulation tool. The simulation tool can, in turn, predict the damage mechanisms of wear, plasticity, and surface RCF crack initiation for different operational conditions.

This emphasizes that the digital twins must provide accurate predictions with fast and memory-efficient simulations, as the numerical simulations for operational traffic should be faster than in real time. Therefore, it is necessary to develop computationally efficient numerical tools such as a reduced order model. Ultimately, the digital twin should serve as a decision-making support tool for rail maintenance, e.g., grinding or replacing rail sections.

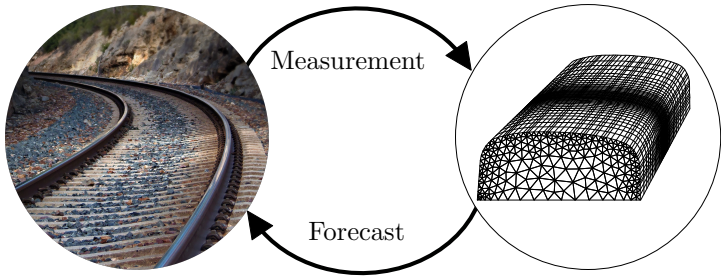

Figure 1.3: *In a digital twin framework, the numerical model is continuously being updated by field measurements to improve the accuracy of the predictions of the material damage in the rail head. Photo from [1].*

The specific objectives of this thesis can be summarized as follows:

- Establish a digital twin framework for a curved rail cross-section, whereby field measurements and simulation results of rail profile changes can be compared.
- Develop a simulation tool that can simulate the development of damage and geometry changes in the rail cross-section for relevant operational traffic and a given rail material. In particular, such a tool requires:
  - Vehicle-track simulations for predicting the load acting on the rail.
  - Simulation of wear on the rail surface.
  - Simulation of the plastic deformation of the rail.
  - Prediction of the propensity to (RCF) crack initiation.
- Improve the numerical efficiency of simulation tools to facilitate fast predictions, in particular by assessing the potential to use the method of Proper Generalized Decomposition for the application of wheel-rail contact.
- Implement model updating in terms of calibrating the adopted models from field measurements.

In this study, the measurements are restricted to geometric changes in the rail cross-section. The prediction of RCF crack initiation is, thus, not compared to field measurements. Another limitation is that the implementation of Proper Generalized Decomposition is conducted as a feasibility study for the simplified case of linear elasticity, whereby it is not adopted in the digital twin framework.

CHAPTER 2

Rail damage in curved tracks

This chapter presents the operational conditions in a field where the test campaign is being conducted. Also, the treatment of measurement data is discussed, and some of the rail profile measurements are shown.

2.1 Operational conditions in the field

A field test campaign is carried out on the western mainline in Sweden, investigating long-term rail profile damage (using a MiniProf measurement device [14]). Specifically, at the location Nyckelsjön and Sparreholmen at three circular curves with curve radii ranging from 1000 to 2000 m.

The curves are exposed to an average of 20 Million Gross Tonnes (MGT) of mixed traffic each year, with 90 % being various passenger vehicles and 10 % freight vehicles. The different types of vehicles have different numbers of wagons and different wheel axle loads. Furthermore, the number of wagons may vary depending on the vehicle configuration, and the wheel axle load is influenced by the number of passengers or freight carried. These are influential factors when it comes to rail damage, because the number of wagons for a vehicle affects the number of overrollings that the rails are subjected to, while a higher wheel axle load results in greater contact forces.

In general, the maximum speed allowed for the vehicles on the train line is 140 km/h [15]. However, the allowed speed is influenced by the maximum absolute lateral acceleration [16] and longitudinal acceleration [17], whereby the permitted speed at the different sites may be reduced. Furthermore, some vehicle types have a tilting system for the car body that reduces the lateral acceleration [18] so that a higher speed can be permitted than

140 km/h.

In addition to the variations in traffic mentioned above, there are several other factors that contribute to rail damage. Environmental conditions, such as rainy days, or when the running surface is covered by ice or leaves, can significantly reduce the wheel-rail friction coefficient, affecting the damage to the rail [3]. Here, also the temperature is important since a high temperature can contribute to track buckling, whereas a low temperature will promote rail breaks. Track irregularities can result in oscillations of the wheelset [19] which may create a contact on the gauge corner on both the left and the right rail and high longitudinal creep forces. This can also promote different damage mechanisms.

2.2 Rail profile measurements

To monitor the condition of rails and detect potential issues before they become problematic, measurements are taken in field to identify damage mechanisms. Various non-destructive methods are used to measure rail damage, such as measuring the rail profile; either using vehicles equipped with laser sensors, or using a handheld device such as the MiniProf, which can detect wear or plastic deformation. Eddy current or ultrasonic measurements can be used to detect cracks.

In this work, the Swedish Transport Administration provided MiniProf (rail instrument from Greenwood Engineering) [14] measurements to obtain field data. Crack detection was not included in the test campaign. Measurements are taken approximately every 60 meters along the three curves and started in May 2021, with new measurements taken every six months. To compare profiles at different times, they are aligned at the field side of the rail using the MiniProf Envision software.

In **Paper A**, field measurements, from two test occasions, were used from a rail curve with a radius of 1974 m. However, two additional measurements have since been performed, but on a different curve since a new rail was installed on the curve used in **Paper A**. Figure 2.1a illustrates a measured cross-section of the outer rail profile taken from the middle of the curved segment for a curve radius of 996 m. Figure 2.1b displays the profile change relative to the cross-section from 2.1a in the normal direction. The Figure displays how the profile change on the inner part of the rail increases between each measurement occasion where the wheel and rail come into contact. The rails were ground before the last measurement occasion (after 30 MGT of traffic load), which can be observed in the Figure since the profile has changed over the entire top part of the rail cross-section.

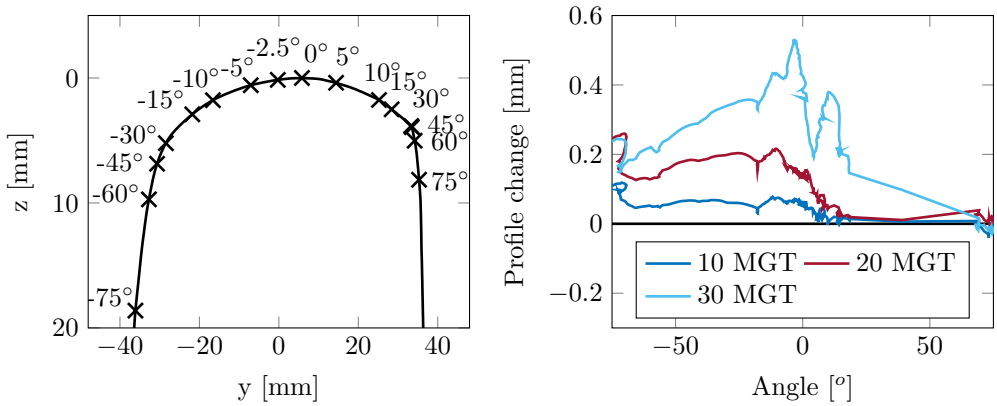

(a) *(b)*

Figure 2.1: *Example measurement of a cross-section of an outer rail head in the middle of the curve for a radius of 996 m. a) displays the coordinates and angles along the rail profile from the first measurement occasion. b) shows the profile change over time in the normal direction relative to the reference cross-sections from the first measurement occasion.*

CHAPTER 3

Numerical modeling to predict rail damage evolution

This chapter presents how long-term rail damage can be evaluated using numerical modeling. The simulation methodology used in this thesis is described and some alternative numerical methods are discussed.

3.1 Simulation methodology

In **Paper A**, a simulation methodology proposed by Skrypnyk et al. [20, 21, 22, 23] to simulate deterioration in switches and crossings is adopted. This methodology can predict the long-term evolution of the rail profile considering cyclic plasticity and wear. The work presented in **Paper A** adapts the simulation framework to the situation of regular curved track and extends the methodology to include an evaluation of surface RCF crack initiation. Figure 3.1 shows the methodology, which consists of four steps and their repetition (iteration). Each iteration includes the following steps:

1. Based on a loading sequence for a given traffic scenario, the dynamic vehicle-track interaction is evaluated using multibody simulations to provide information on the position and magnitude of the contact forces.
2. Analyzing the normal wheel-rail contact problem using a metamodel inspired by Hertz's contact method [24] for each contact scenario in the loading sequence, considering elastic-plastic material of the rail and elastic material of the wheel. This simulation calculates the size of the contact area and the stress level.
3. The load sequence can be repeated to generate a load collective in each iteration of the methodology. For this load collective, the rail damage predicted as follows:

(a) Computation of accumulated plastic deformation for load cases with high contact loads using nonlinear 2D FE simulations with cyclic plastic material. The normal contact load is adjusted for each load case to achieve the same maximum value of von Mises stress obtained from the Hertzian metamodel in step 2.

(b) Simulation of wear based on Archard's wear model [25] combined with a FASTSIM [26] discretization of the contact area.

(c) Computation of a distributed fatigue damage index is used to predict crack initiation due to surface RCF. The index used was proposed by Nielsen et al. [27] and is based on the shakedown theory [28], but takes into account partial slip and interaction with wear.

4. The rail profile is updated due to the accumulative effect of plastic deformation and wear. The updated rail profile is used as input for the dynamic simulation in step 1 of the next iteration of the simulation methodology.

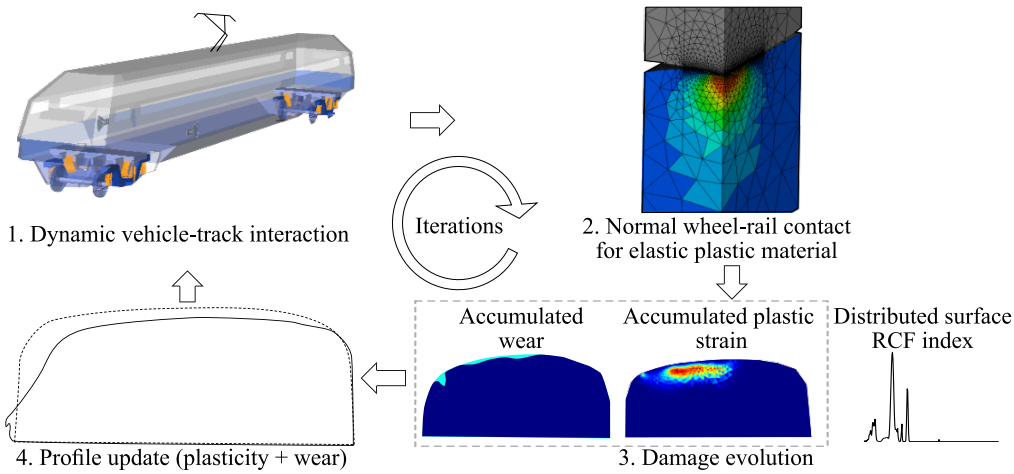

Figure 3.1: *Illustration of iterative simulation methodology for rail damage prediction. 1. dynamic vehicle model for each wagon in the loading sequence to evaluate the dynamic vehicle-track interaction; 2. 3D analysis of the elastic-plastic normal contact for each contact scenario in the loading sequence based on a Hertzian-inspired metamodel; 3. 2D prediction of plastic deformation, wear, and surface RCF index of the rail head due to cyclic loading; 4. profile update of the rail due to plasticity and wear.*

The iteration steps are repeated until the desired amount of traffic has been simulated. A load collective is generated because it is computationally intensive to update the rail profile after each wheel pass. The traffic scenario aims to capture the field operating conditions described in Section 2.1 by accounting for variations in wheel profiles, vehicle speed, and axle loads.

Both the computation of wear and evaluation of RCF import the contact forces directly from the multibody simulations in step 1, i.e., they are not obtained from the metamodel

in step 2.

In **Paper B**, steps 1 and 3b are performed for one load sequence to investigate influential model parameters that affect local wear on a rail head in a curved track. The traffic scenario is updated for different model parameters related to the vehicle or the track. Also, different wheel-rail contact models are used to estimate the local wear. These contact models were modified in the multibody simulations in step 1 or by using a combination of the initial contact model in the multibody simulations but combining it with the Hertzian-inspired metamodel from step 2.

A reduced order model called Proper Generalized Decomposition (PGD) is initialized in **Paper C** to improve efficiency and accuracy of simulations in the digital twin framework. It is implemented for a 3D elastic rail for different loading scenarios. The different contact scenarios from the loading sequence are given from the dynamic vehicle-track interaction described in step 1, but consider a different wheel-rail contact model than the one used in **Paper A**. This implementation is a first step toward enhancing the numerical model of accumulated plasticity described in step 3a to reduce computational costs while improving accuracy as the 3D problem is solved. In addition, with the PGD model, it is possible to consider the interaction when there are multiple contact points for a wheel overrolling.

The following sections contain a more detailed description of the individual steps.

3.2 Wheel-rail contact models

It is essential to accurately capture the shape, magnitude, and distribution of contact stresses in the wheel-rail contact to evaluate rail head degradation in numerical modeling.

3.2.1 Preliminaries

In general, normal and tangential tractions are not independent of each other. However, as shown in [29], the tangential contact traction for elasticity does not have a large effect on either the normal contact pressure distribution nor the contact area size. Therefore, the normal contact is first computed to determine the contact area, and the magnitude and distribution of the normal contact pressure. Using the results of the normal contact and the creepages, the shear stresses for the tangential contact can be determined. The resulting stress is superimposed by the contact pressure and the tangential traction.

Several methods with varying degrees of complexity and accuracy are available to solve the normal contact problem. In their extensive review, Meymand et al. [30] discussed commonly used approaches such as the Hertz contact method [24] and Kalker's CONTACT program [31, 32]. Additionally, they presented other contact theories that were inspired by the Hertzian contact, such as a multi-Hertzian model proposed by Piotrowski and Chollet [33] and a virtual penetration model showcased in Hashemi and Paul [34], among others. In this thesis, we restrict ourselves to consider the contact models that are already available in the simulation methodology presented by Skrypnyk et al. [20, 21, 22, 23], or those that are available in the multibody simulation software Simpack.

The following contact models are assessed:

- Hertzian theory of contact [24].
- Semi-Hertzian model called STRIPES in [35, 36]. Here, the tangential contact is considered with a modified FASTSIM [26] algorithm.
- Hertzian inspired metamodel [20].

The tangential problem is typically solved by often using the FASTSIM algorithm [26]. These different contact methods are described in the following sections.

3.2.2 Hertzian theory of contact

For modeling normal wheel-rail contact, Hertz contact theory [24] is commonly used because of its simplicity and rapidity. According to Hertz, an elliptical contact patch is formed when two bodies are pressed against each other with a normal force. The Hertzian pressure distribution $p(x, y)$ in the elliptical area with semi-axes a and b is

$$p(x,y) = p_0\sqrt{1-\left(\frac{x}{a}\right)^2-\left(\frac{y}{b}\right)^2}, \quad |x|<a, \quad |y|<b, \tag{3.1}$$

where x and y are coordinates within the elliptical area and p_0 is the maximum pressure. Figure 3.2 displays an elliptical contact area and the pressure distribution for a Hertzian contact.

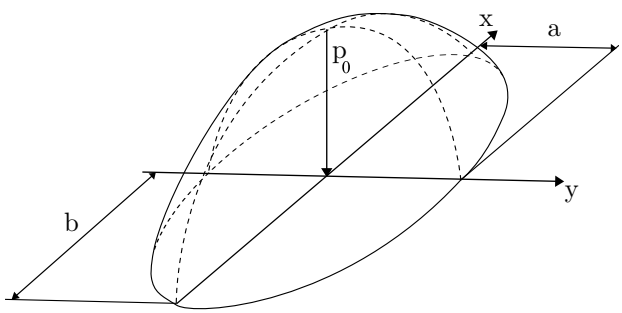

Figure 3.2: *Hertz contact showing the semi-axes a and b and how the normal pressure is distributed from p_0.*

For the Hertzian contact to be valid, the following assumptions must be true:

1. The material of the contacting bodies behaves linearly elastic, indicating small displacements and strains.
2. The bodies are nonconforming, i.e., the contact area (a and b) is much smaller than the dimensions and radii of the contacting bodies. This is called the *half-space assumption*.
3. Surfaces in the contact area can be described by constant curvatures.

In many contact scenarios, these assumptions are more or less valid. However, one or more of these assumptions are violated when there is high contact pressure, flange contact on the wheel, or irregularities on the wheel or rail profile. At high contact pressure, plastic deformation can occur, violating the first assumption. In the case of flange contact, the second assumption is violated because the contact is conformal if the lateral radius of the wheel flange is in the same range as the size of the contact area. In addition, Hertz's contact theory cannot handle two-point contacts, which are common in curves. Moreover, the third assumption is usually violated since real rail and wheel profiles do not have constant curvatures, especially in the lateral direction.

3.2.3 STRIPES

Due to the limitations of Hertz's contact theory, there are scenarios when Hertz's contact theory is inadequate. Therefore, Ayesse et al. [35], and Quost et al. [36], have proposed a semi-Hertzian approach called STRIPES, which is more precise but still computationally efficient. This method estimates the contact area from the interpenetration area, which refers to the virtual penetration of undeformed surfaces. The contact area is then split into $m = 1, ..., M$ discrete strips of width Δy parallel to the direction of rolling, as illustrated in Figure 3.3. In each strip, the normal stress distribution is determined by applying a Hertzian-based formula in the direction of rolling. Therefore, the curvature is locally constant in the longitudinal direction, but it allows for a non-constant curvature in the lateral direction. To solve the tangential problem in STRIPES, a modified FASTSIM algorithm [26] is employed, cf. below.

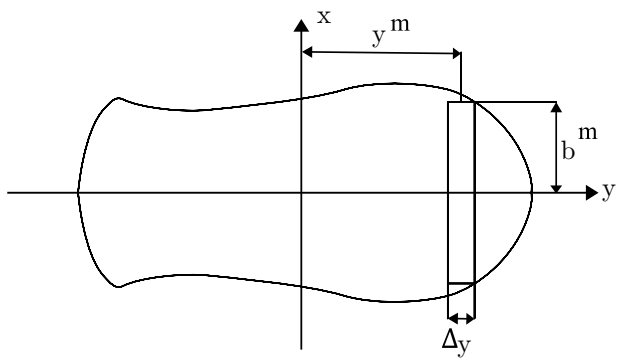

Figure 3.3: *An example of contact area using STRIPES contact method, where x defines the rolling direction of the contacting wheel. The contact patch is divided into $m = 1, ..., M$ discrete strips. The figure shows the width of the strip Δy, its position along the y-axis y^m, and its semi-axis b^m.*

3.2.4 Hertzian-inspired metamodel

Skrypnyk et al. [20] presented a metamodel for the normal contact problem that is inspired by Hertz's contact theory while considering elastic-plastic material behavior in the rail and elastic material behavior of the wheel. The model uses the local contact radii and normal contact force as inputs to predict the size of the contact patch, the maximum contact pressure, and the maximum von Mises stress.

A metamodel is a simplified model used to replace more complex models to reduce computational costs. It is called a "meta" model because it is itself a model of another model. To determine the model coefficients, a large reference dataset is required. For the Hertzian-inspired metamodel for normal wheel-rail contact used in **Paper A**, the reference dataset contains results from 3D Finite Elements (FE) normal contact simulations for a specified range of contact scenarios that consider the elastic-plastic behavior of the rail material. Since the curvatures of the radii of the rail and wheel are assumed to be constant near the contact point (as in Hertz's contact theory), the contact patch is symmetric. As a result, only a quarter of the contact patch is simulated in the FE simulations, illustrated for step 2 in Figure 3.1.

Rather than simulating each new contact with FE modeling, the metamodel can use the few calibrated model coefficients to provide accurate results with almost no computational time while considering the elastic-plastic material behavior. However, the metamodel has a limitation in that it assumes constant curvature radii when producing the reference data set.

3.2.5 FASTSIM

Tangential forces arise if the wheelset is not rolling ideally on the track since sliding occurs in the contact. This is more or less always the case in railway vehicles since the suspension prevents the wheelset from pure rolling. However, the creepages can become greater during acceleration, braking, or on curved tracks.

The contact patch can be split into two regions, namely, the stick and the slip regions, as shown in Figure 3.4, cf. [29]. In the stick region of the contact area, there is no relative motion between the bodies, while in the slip region, the bodies slide relative to each other. As the relative velocities or creepages in the contact increase, the slip portion increase, and the resulting traction stress $q(x, y)$ reaches a limit determined by Coulomb's law, which is the product of normal pressure $p(x, y)$ and friction coefficient μ.
Kalker has proposed several theories to describe tangential contact, ranging from simplified to more exact ones [37]. Nowadays, tangential contact is typically solved using Kalker's simplified contact theory (FASTSIM) [26] due to its low computational cost. In FASTSIM, the contact area is discretized into $n_{\mathrm{x}} \times n_{\mathrm{y}}$ rectangular elements with element size $\Delta x \times \Delta y$. In each element, the tangential traction is computed. In FASTSIM, the displacement of the surface is proportional to the traction and the traction stresses reach a value limited by Coulomb's law. Although FASTSIM is originally applied to solve the tangential contact problems for Hertz theory, it can also be modified for other contact methods such as for the STRIPES method discussed in Section 3.2.3.

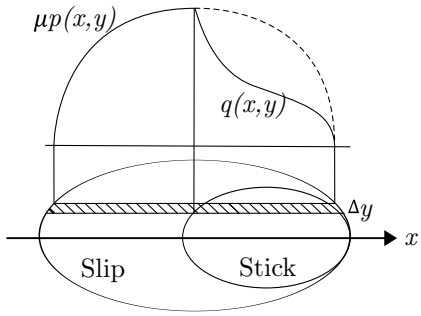

Figure 3.4: *Tangential traction distribution in an elliptical contact. The tangential traction stress $q(x, y)$ is limited by Coulomb's law $\mu p(x, y)$.*

3.3 Dynamic vehicle-track interaction

Commercial software tools such as GENSYS [38] or Simpack [39] can be used for multibody simulations of the dynamic vehicle-track interaction. In this thesis, Simpack is utilized to generate load sequences for various traffic scenarios in the time domain. The simulations provide information regarding the contact locations, wheel-rail contact forces, and creepages that are used for computing the normal contact problem using the Hertzian-inspired metamodel and computing damage. In Simpack, a maximum of five contact points can be present simultaneously. However, in the subsequent steps in the simulation methodology, the contact points are treated separately.

Two different methods can be used to model contact in the dynamic-vehicle track interaction. The first method involves solving the normal contact using the equivalent elastic contact model, based on Hertz's contact theory [24], and solving the tangential contact using the FASTSIM algorithm [26]. The second method uses the discrete elastic contact method that employs the semi-Hertzian approach STRIPES [35, 36]. In STRIPES, the tangential contact is solved using a modified FASTSIM algorithm [26]. The discrete elastic-plastic contact method considers the influence of ideal elastic-plastic material behavior, resulting in a reduction in contact stresses and changes in the contact area due to the plastic flow of the material [40, 41]. This is achieved by reducing the normal force contribution of the individual slices in such a way that they do not exceed the normal force resulting from an ideal elastic-plastic material.

3.4 Cyclic plasticity material model

To predict the profile changes due to plastic deformation, it is crucial to use a material model that can describe the cyclic plastic behavior of the rail material. Ohno-Wang [42] is a cyclic nonlinear plasticity model that assumes small strains, linear isotropic elasticity, the von Mises yield function, and accounts for nonlinear kinematic hardening. The nonlinear evolution of the backstress $\dot{\boldsymbol{\alpha}}_i$ representing the kinematic hardening is

proposed by Ohno-Wang [42] as

$$\dot{\boldsymbol{\alpha}}_i = \frac{2}{3}\, C_i\, \dot{\boldsymbol{\epsilon}}^{\mathrm{p}} - \frac{\gamma_i^{m_i+1}}{C_i^{m_i}} \left(\sqrt{\frac{3}{2}} |\boldsymbol{\alpha}_i| \right)^{m_i} < \dot{\boldsymbol{\epsilon}}_{\mathrm{p}} : \boldsymbol{\alpha}_i > \sqrt{\frac{2}{3}} \frac{\boldsymbol{\alpha}_i}{|\boldsymbol{\alpha}_i|}, \tag{3.2}$$

where $\dot{\boldsymbol{\epsilon}}^{\mathrm{p}}$ is the evolution of plastic strain, C_i is the hardening modulus of each backstress i, m_i represents a multiplier and the exponent γ_i is a model parameter. The number of backstresses used depends on how many are necessary to fit model behavior sufficiently well to the experimental data. The sum of the backstresses gives the center of the yield surface in stress space. For more information on this material model we refer to Brommesson et al. [43].

In **Paper A**, the material model was calibrated against two uniaxial stress-controlled experimental data from test specimens of rail grade R260 by Ahlström et al. [44], including three backstresses. The calibrated values of the material parameters are listed in **Paper A**. In the simulation methodology of this paper, this material model is used to account for the elastic-plastic material response in the Hertzian-inspired metamodel. Furthermore, the same material model is employed to evaluate rail damage when it comes to the accumulation of plastic deformation.

3.5 Simulation of damage mechanisms

To estimate the total damage to the rail, we consider accumulated plastic deformation, wear, and surface RCF. Although the damage mechanisms interact with each other, many computation techniques decouple the interaction for simplicity.

3.5.1 Accumulated plastic deformation

Efficient simulations are essential for estimating the accumulated plastic deformation in a rail subjected to many loading cycles. To reduce the computational effort, this thesis employs 2D non-linear FE-models of the studied rail cross-sections to predict the accumulated plastic deformation, assuming small strains. To make the 2D simulations more accurate, the maximum normal force per unit length is adjusted as a pre-processing step for each loading case to achieve the same maximum von Mises stress as the 3D Hertzian-inspired metamodel. Plasticity is then computed for the 2D cross-section, accounting for tangential traction by assuming full slip. The load cycles in the plasticity simulation are extrapolated using a procedure explained in [45] to save computational time.

In **Paper A**, the measured rail profiles were dominated by wear, allowing for the extrapolation of many load cycles. However, in order to obtain agreement between the rail profile measurements and simulations in terms of the isochoric area (cf. **Paper A**), the yield limit of the material is changed. This is necessary because the material in the field has been more work-hardened compared to the specimen material that the plasticity model was calibrated for.

3.5.2 Wear

Wear is usually estimated using, (a) models relating wear to frictional energy [46], or (b) Archard-based models for sliding wear [25]. In this thesis, Archard's wear law is used.

To obtain a distribution of wear in the contact area, Archard's wear law can be used in conjunction with the FASTSIM [26] discretization of the contact area. The wear depth distribution $\Delta z(x, y)$ can then be written as

$$\Delta z(x, y) = k_{\mathrm{w}} \frac{p(x, y) \Delta d(x, y)}{H}, \tag{3.3}$$

where $p(x, y)$ is the normal contact stress given from (3.1) and $\Delta d(x, y)$ is the slip distance in each element of the discrete contact area given from the dynamic vehicle-track interaction simulations. The hardness of the softer of the two contacting materials is H and the wear coefficient k_{w} depends on the stresses and the sliding velocity in the contact area. A detailed description can be found in [27].

Both the frictional energy models and Archard-based models for sliding wear have wear rates depending on coefficients (k_{w} in Archard's wear law) that are specific to the loading conditions and can vary along the rail profile. To address this, a wear map can be constructed for different contact pressures and sliding velocities, as shown in the work of Olofsson and Telliskivi [7]. However, wear maps are material-specific and require extensive testing. In addition, wear maps are created for specific operational conditions, which may be completely different from those in the considered field tests. For this reason, the wear coefficient is calibrated in **Paper A** to obtain a good agreement between the rail profile measurements and the simulations in terms of the worn area (cf. **Paper A**). In **Paper A**, a constant wear coefficient value is used throughout the rail profile. The same value for the wear coefficient is also considered in **Paper B**.

3.5.3 Surface rolling contact fatigue

Ekberg and Kabo [47] presented several models to predict surface-induced Rolling Contact Fatigue (RCF). One such model is the shakedown map based on the Hertzian theory [28, 48], which predicts where surface plasticity occurs and relates ratcheting to RCF crack initiation. To improve the accuracy of contact stress predictions, elastic-plastic material behavior of the contacting surface can be incorporated through FE modeling [49]. Alternatively, simpler models based on contact pressure can be employed. Combining a multiaxial low-cycle fatigue criterion [50] and a ratcheting criterion [13] has also proven to be successful.

In this thesis, surface RCF crack initiation is predicted using a distributed RCF index, proposed by Nielsen et al. [27]. The index is based on the shakedown theory [28], but accounts for partial slip and interactions with wear. The RCF index of the distributed surface is related to the energy dissipation T_γ (but neglecting spin) to capture the interaction with wear. Therefore, a penalty function $f_{\mathrm{p}}(T_\gamma)$ is employed to reduce the surface index at higher values of T_γ, as high energy dissipation results in high wear rate and worn-off cracks [51]. The turning points in the penalty function are determined based on the contact area and material properties of the rail grade. To account for partial slip, the local damage is computed for each rectangle in the contact area discretization using

the FASTSIM [26] output. The index estimates the risk of crack initiation from passing vehicles and is accumulated using the Palmgren-Miner rule, indicating crack initiation when the index reaches a value of 1. The proposed approach provides an estimation of the risk of crack initiation, accounting for various factors affecting the phenomenon.

3.6 Model reduction

Reduced order modeling is a technique utilized to reduce the computational complexity of a model. Proper Orthogonal Decomposition (POD) [52, 53], Reduced Basis (RB) [54], and Proper Generalized Decomposition (PGD) are some examples of available methods for model reduction. While POD and RB require knowledge of the (approximate) solution to the complete problem, PGD is an a priori technique that does not [55]. As such, PGD will be used in this thesis. In PGD, a successive enrichment strategy is used to obtain a numerical approximation of the unknown fields in a separate form. For instance, we can seek a solution for the unknown field $u(x^1, ..., x^{\mathrm{M}})$ using the PGD separated representation, also known as a finite-sum decomposition, as

$$u(x^1, ..., x^{\mathrm{M}}) \approx u_{\mathrm{N}}^{\mathrm{pgd}}(x^1, ..., x^{\mathrm{M}}) = \sum_{i=1}^{N} \prod_{m=1}^{\mathrm{M}} F_i^m(x^m), \tag{3.4}$$

where N represents the number of unknown terms and $F_i^m(x^m)$ denotes the unknown functions for the coordinates x^m in the space dimension M. Here, x^m can represent spatial coordinates (x, y, z) and/or general parameters, e.g. load parameters.

After calculating the offline solution of the separated representation of the parametric solution, the online solution can be determined. The offline solution is solved only once and includes all solutions of the parameters within their respective intervals. For the online phase, a particular solution to the problem can be efficiently obtained at low cost. This requires only a post-processing step of the pre-computed parametric solution for a desired setup of the parameter values.

The PGD method can be applied to a wide variety of problems, such as high-dimensional problems, parametric modeling with large sets of parameters, or when a very fast solution is required.

In **Paper C**, a domain decomposition was introduced for the 3D elastic rail head as proposed in [56, 57] by modeling the rail cross-section in 2D and treating the coordinate along the rail as a parameter in the separated representation. This allows the full 3D model to be solved with 2D computational effort. Furthermore, a discrete surface load described with STRIPES [35, 36] was also considered as parameters in the PGD approximation, The extra dimension of the problem does not affect the solvability, although more terms are needed to accurately capture the solution.

CHAPTER 4

Summary of appended papers

A summary of the appended papers is given in this chapter.

Paper A

> C. Ansin, B. Pålsson, M. Ekh, F. Larsson and R. Larsson, "Simulation and field measurements of the long-term rail surface damage due to plasticity, wear and surface rolling contact fatigue cracks in a curve". *Proceedings 12th International Conference on Contact Mechanics and Wear of Rail/Wheel Systems (CM2022)*, Melbourne (Australia) September 2022, 11 pp.

Paper A presents numerical simulations to predict the long-term rail surface damage in a rail cross-section in a curved track for a given traffic scenario. The used simulation methodology is calibrated and validated using field tests. The numerical methodology includes multiple steps iteratively applied: dynamic vehicle-track interaction for a given loading situation, elastic-plastic wheel-rail contact, and rail damage from cyclic plasticity, surface wear, and initiation of RCF surface cracks. The rail profile is updated from the accumulated wear and plasticity, and the simulation steps can be repeated. Also, a surface criterion for RCF crack initiation is evaluated. The computational cost of accounting for many load cycles is intensive. To reduce the computational cost, nonlinear 2D FE simulations with cyclic plastic material are used to compute accumulated plastic deformation. Also, the loading cycle is repeated several times before the dynamic vehicle-track interaction is computed again, where some of the loading cycles are extrapolated in the plasticity simulation.

From the results, it is shown how the numerical model can predict surface RCF crack initiation, and be calibrated to fit field measurements of the average geometry changes of the rail cross-section, which includes the worn and isochoric (corresponding to plastic deformation) cross-sectional area. However, Figure 4.1 shows that the damage distributions between the field measurement and simulation differ, especially at the flange contact. The discrepancies can be caused by several factors. Firstly, the curve was not subjected to significant traffic between the two measurement occasions with a profile change of a few tenths of a millimeter, making them sensitive to measurement errors. Secondly, the use of Hertz contact theory to model normal contact may oversimplify the contact conditions. Finally, there may be limitations in the representation of the traffic load compared to actual field conditions.

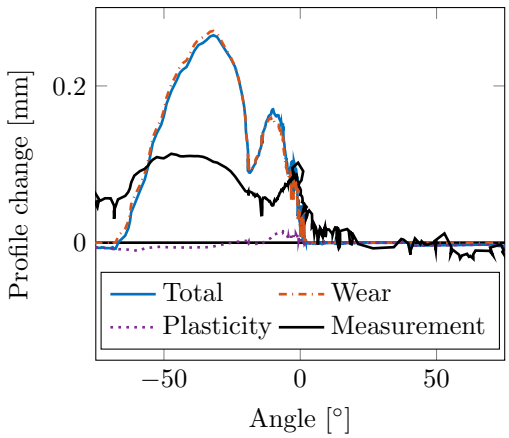

Figure 4.1: *Profile change in the normal direction of one cross-section. The result display both the profile change for the measurement as well as the simulation after approximately 10 MGT of traffic. The figure, also displays how the profile has changed due to wear and plasticity.*

Paper B

C. Ansin and B. Pålsson. "Influence of model parameters on the predicted rail profile wear distribution in a curve". *Internal report, Chalmers University of Technology, 2023.*

Paper B is an extension to **Paper A** with the aim of exploring the influence of model parameters on the predicted rail profile wear distribution in a curved track. To achieve this, multibody simulations are used to analyze the dynamic vehicle-track interaction under various traffic scenarios. Archard's wear law [58] in conjunction with the FASTSIM [26] discretization is used to assess the wear on the rail surface. The objective of **Paper B** is to investigate the sensitivity of vehicle and track parameters on the local surface

damage. Also, different approaches to contact modeling are considered. The results in **Paper B** indicate that considering freight vehicles, exploring a different set of wheel profiles, and selection of a contact model are some of the most significant parameters.

Paper C

> C. Ansin, F. Larsson and R. Larsson. "Fast Simulation of 3D Elastic Wheel-Rail Contact Using Proper Generalized Decomposition". *Manuscript to be submitted for publication.*

Paper C implements a reduced order model based on the Proper Generalized Decomposition (PGD) method for a three-dimensional rail head with elastic material properties subjected to different contact scenarios. Initially, the 3D solid rail is decomposed such that the rail cross-section is modeled in two dimensions, while the coordinate along the rail is a parameter in the PGD approximation. The results are promising compared to traditional 3D FE simulations for a fixed Hertzian load. The PGD model can produce accurate results with 2D computational complexity, resulting in large savings in computational cost and memory allocation compared to 3D FE simulations, see Figure 4.2.

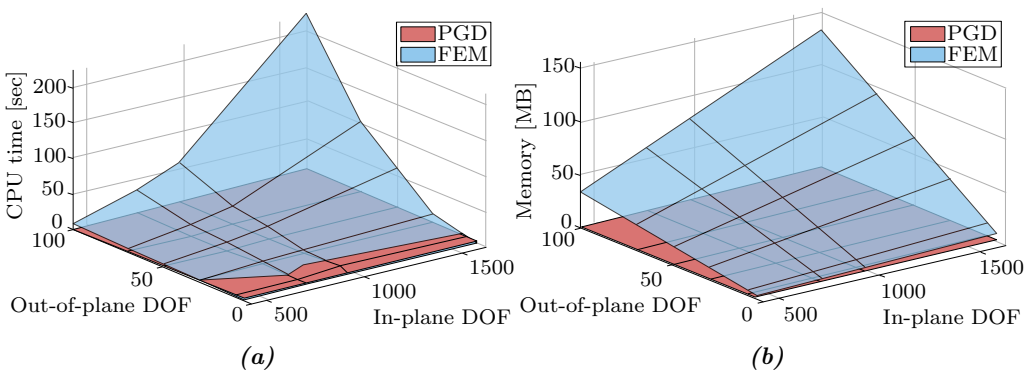

Figure 4.2: *Comparisons of (a) Central Processing Unit (CPU) time and (b) memory allocation between PGD and 3D FE simulation for different in- and out-of-plane discretizations.*

The subsequent step involves the inclusion to parameterize the distributed load for different contact locations as extra-coordinates in the PGD formulation by utilizing the STRIPES method [35, 36], which is a semi-Hertzian approach. In STRIPES, the load distribution in the lateral direction is discretized as a piece-wise constant while a parabolic distribution is assumed along the rolling direction. For each added strip, additional parameters are introduced into the PGD approximation. In this way, we can represent a large number of contact scenarios with independent normal and tangential stress distribution. In addition, multiple contact points can be active simultaneously. Therefore, the PGD formulation must be able to handle many parameters. For every added strip, the model's complexity increases, and the efficiency of generating the solution decreases since more

modes must be considered. Nonetheless, a single solution for the displacement field can be generated for any choice of load parameters within the space. Thus, we can allow for a computationally expensive offline solution, as the online solution is a post-processing step that is computationally inexpensive to generate for a specific setup of the load parameters.

CHAPTER 5

Conclusions and outlook

The goal of this research is to take steps towards a digital twin that can predict the rail head damage evolution in curved tracks while considering field operational conditions. To achieve this, fast numerical simulations are conducted as discussed in Chapter 3 alongside updates based on the field measurements, which are briefly outlined in Chapter 2.

In **Paper A**, the long-term damage and evolution of a rail in a curved track for operational traffic were examined using numerical simulations and field measurements. The numerical framework involves multiple steps applied in an iterative scheme between (1) dynamic vehicle-track interaction for a given loading situation, (2) elastic-plastic wheel-rail contact, (3) accumulative rail damage, which considers plasticity, wear, and surface RCF crack initiation, and (4) the rail profile is updated from the accumulative wear and plasticity, and the simulation steps can be repeated for that rail geometry. It was demonstrated that the numerical model can be calibrated to match field measurements of average changes in rail cross-section geometry. To further improve the prediction of local damage of a cross-section, a sensitivity study of the model was conducted in **Paper B** to determine the most influential model parameters. It was found that considering a different contact model, using a different set of measured wheel profiles, and including a freight vehicle in the traffic scenario gives results that match better with the field data.

A reduced order model based on the Proper Generalized Decomposition (PGD) was developed in **Paper C** to allow for cost-efficient simulations in the rail for the simplified case of linear elasticity. This is necessary to obtain a feasible digital twin framework that in the future accounts for plasticity evolution. For the current version, a domain decomposition for the 3D elastic rail head was introduced by modeling the rail cross-section in 2D and treating the coordinate along the rail as a parameter in the separated representation. The distributed surface load for different contact locations is treated as

extra-coordinates in the PGD formulation. It was shown that the implementation of the PGD accurately reproduces the deformation of the rail for the simplified assumptions of elastic material behavior and a semi-Hertzian contact.

Some questions remain for the work presented in this thesis. The continuation of this work can be divided into the following parts:

- Implement elastic-plastic material behavior of the rail in the reduced order model.
- Introduce the reduced order model into the simulation framework presented in **Paper A**.
- Consider additional field data in the model calibration to improve the predictions of the numerical model and to get a better understanding of the damage in the field.
- Implement some of the influential model parameters from the model sensitivity study into the load sequence for the long-term prediction of rail profile change.

Additionally, one could consider developing the reduced order model such that it can be used as a contact model in a multibody simulation tool for efficient simulations while accounting for detailed geometric and material effects.

References

[1] *Free Images : track, railway, train, travel, curve, vehicle, lane, locomotive, infrastructure, trains, dreams, destination, rail transport, waiting for you, pathways, rolling stock 4288x3216 - - 1086051 - Free stock photos - PxHere*. en.

[2] E. E. Magel. *Rolling Contact Fatigue: A Comprehensive Review*. English. Nov. 2011.

[3] A. Ekberg and E. Kabo. "Key parameters and requirements for track health prediction". en. In: (), p. 71.

[4] A. Kapoor, I. Salehi, and A. M. S. Asih. "Rolling Contact Fatigue (RCF)". en. In: *Encyclopedia of Tribology*. Ed. by Q. J. Wang and Y.-W. Chung. Boston, MA: Springer US, 2013, pp. 2904–2910. DOI: 10.1007/978-0-387-92897-5_287.

[5] K. A. Meyer, D. Nikas, and J. Ahlström. "Microstructure and mechanical properties of the running band in a pearlitic rail steel: Comparison between biaxially deformed steel and field samples". en. In: *Wear* 396-397 (Feb. 2018), pp. 12–21. DOI: 10.1016/j.wear.2017.11.003.

[6] K. Karttunen. "Influence of rail, wheel and track geometries on wheel and rail degradation". en. In: (2012).

[7] U. Olofsson and T. Telliskivi. "Wear, plastic deformation and friction of two rail steels—a full-scale test and a laboratory study". en. In: *Wear* 254.1 (Jan. 2003), pp. 80–93. DOI: 10.1016/S0043-1648(02)00291-0.

[8] D. F. Cannon and H. Pradier. "Rail rolling contact fatigue Research by the European Rail Research Institute". en. In: *Wear*. 4th International Conference on Contact Mechanics and Wear of Rail-Wheel Systems 191.1 (Jan. 1996), pp. 1–13. DOI: 10.1016/0043-1648(95)06650-0.

[9] W. J. Wang et al. "Investigation on the damage mechanism and prevention of heavy-haul railway rail". en. In: *Engineering Failure Analysis*. Special issue on ICEFA V-Part 1 35 (Dec. 2013), pp. 206–218. DOI: 10.1016/j.engfailanal.2013.01.033.

[10] M. Schilke, N. Larijani, and C. Persson. "Interaction between cracks and microstructure in three dimensions for rolling contact fatigue in railway rails". en. In: *Fatigue & Fracture of Engineering Materials & Structures* 37.3 (2014), pp. 280–289. DOI: 10.1111/ffe.12112.

[11] A. Ekberg and P. Sotkovszki. “Anisotropy and rolling contact fatigue of railway wheels”. en. In: *International Journal of Fatigue* 23.1 (Jan. 2001), pp. 29–43. DOI: 10.1016/S0142-1123(00)00070-0.

[12] N. Larijani et al. “The effect of anisotropy on crack propagation in pearlitic rail steel”. en. In: *Wear*. Proceedings of the 9th International Conference on Contact Mechanics and Wear of Rail / Wheel Systems, Chengdu, 2012 314.1 (June 2014), pp. 57–68. DOI: 10.1016/j.wear.2013.11.034.

[13] A. Kapoor. “A Re-Evaluation of the Life to Rupture of Ductile Metals by Cyclic Plastic Strain”. en. In: *Fatigue & Fracture of Engineering Materials & Structures* 17.2 (1994), pp. 201–219. DOI: 10.1111/j.1460-2695.1994.tb00801.x.

[14] *MiniProf Envision*. en-US.

[15] M. Edlund. *Underlag till linjebok*. sv. Tech. rep. Trafikverket, Nov. 2021, p. 437.

[16] *Tillåten hastighet m.h.t. spårets geometriska form. BVF 586.41*. Swedish. 1996.

[17] E. Andersson et al. *Rail Systems and Rail Vehicles : Part 2: Rail Vehicles*. eng. KTH Royal Institute of Technology, 2016.

[18] E. Andersson, M. Berg, and S. Stichel. *Rail Vehicle Dynamics*. Swedish. Stockholm: Centre for Research and Education in Railway Engineering, Railway Group KTH, 2007.

[19] K. Karttunen, E. Kabo, and A. Ekberg. “The influence of track geometry irregularities on rolling contact fatigue”. en. In: *Wear*. Proceedings of the 9th International Conference on Contact Mechanics and Wear of Rail / Wheel Systems, Chengdu, 2012 314.1 (June 2014), pp. 78–86. DOI: 10.1016/j.wear.2013.11.039.

[20] R. Skrypnyk et al. “Metamodelling of wheel–rail normal contact in railway crossings with elasto-plastic material behaviour”. en. In: *Engineering with Computers* 35.1 (Jan. 2019), pp. 139–155. DOI: 10.1007/s00366-018-0589-3.

[21] R. Skrypnyk et al. “Prediction of plastic deformation and wear in railway crossings – Comparing the performance of two rail steel grades”. en. In: *Wear* 428-429 (June 2019), pp. 302–314. DOI: 10.1016/j.wear.2019.03.019.

[22] R. Skrypnyk et al. “Long-term rail profile damage in a railway crossing: Field measurements and numerical simulations”. en. In: *Wear* 472-473 (May 2021). DOI: 10.1016/j.wear.2020.203331.

[23] R. Skrypnyk et al. “On the influence of crossing angle on long-term rail damage evolution in railway crossings”. In: *International Journal of Rail Transportation* 9.6 (Jan. 2021), pp. 503–519. DOI: 10.1080/23248378.2020.1864794.

[24] H. Hertz. “On the contact of solid, elastic bodies”. In: *Journal für die reine und angewandte Mathematik* 92 (1882), pp. 156–171.

[25] J. F. Archard. “Contact and Rubbing of Flat Surfaces”. In: *Journal of Applied Physics* 24.8 (Aug. 1953). Publisher: American Institute of Physics, pp. 981–988. DOI: 10.1063/1.1721448.

[26] J. Kalker. “A Fast Algorithm for the Simplified Theory of Rolling Contact”. In: *Vehicle System Dynamics* 11.1 (Feb. 1982), pp. 1–13. DOI: 10.1080/00423118208968684.

[27] J. C. O. Nielsen, B. A. Pålsson, and P. T. Torstensson. “Switch panel design based on simulation of accumulated rail damage in a railway turnout”. en. In: *Wear*. Contact Mechanics and Wear of Rail / Wheel Systems, CM2015, August 2015 366-367 (Nov. 2016), pp. 241–248. DOI: 10.1016/j.wear.2016.06.021.

[28] K. Johnson. “The strength of surfaces in rolling contact”. English. In: *Proceedings of the Institution of Mechanical Engineers, Part C: Journal of Mechanical Engineering Science* 203.3 (May 1989), pp. 151–163. DOI: 10.1243/PIME_PROC_1989_203_100_02.

[29] K. L. Johnson. *Contact Mechanics*. en. Cambridge University Press, Aug. 1987.

[30] S. Z. Meymand, A. Keylin, and M. Ahmadian. “A survey of wheel–rail contact models for rail vehicles”. In: *Vehicle System Dynamics* 54.3 (Mar. 2016). Publisher: Taylor & Francis _eprint: https://doi.org/10.1080/00423114.2015.1137956, pp. 386–428. DOI: 10.1080/00423114.2015.1137956.

[31] J. J. Kalker. *Three-Dimensional Elastic Bodies in Rolling Contact*. en. Google-Books-ID: DBLiT7I4qEQC. Springer Science & Business Media, Oct. 1990.

[32] J. J. Kalker. “Wheel-rail rolling contact theory”. en. In: *Wear* 144.1 (Apr. 1991), pp. 243–261. DOI: 10.1016/0043-1648(91)90018-P.

[33] J. Piotrowski and H. Chollet. “Wheel–rail contact models for vehicle system dynamics including multi-point contact”. In: *Vehicle System Dynamics* 43.6-7 (June 2005). Publisher: Taylor & Francis _eprint: https://doi.org/10.1080/00423110500141144, pp. 455–483. DOI: 10.1080/00423110500141144.

[34] J. Hashemi and B. Paul. “Contact stresses on bodies with arbitrary geometry, applications to wheels and rails”. In: (Apr. 1979). Number: MEAM-79-2.

[35] J. Ayasse and H. Chollet. “Determination of the wheel rail contact patch in semi-Hertzian conditions”. In: *Vehicle System Dynamics* 43.3 (Mar. 2005). Publisher: Taylor & Francis _eprint: https://doi.org/10.1080/00423110412331327193, pp. 161–172. DOI: 10.1080/00423110412331327193.

[36] X. Quost et al. “Assessment of a semi-Hertzian method for determination of wheel–rail contact patch”. In: *Vehicle System Dynamics* 44.10 (Oct. 2006). Publisher: Taylor & Francis _eprint: https://doi.org/10.1080/00423110600677948, pp. 789–814. DOI: 10.1080/00423110600677948.

[37] K. Zaazaa and A. Schwab. “Review of Joost Kalker’s Wheel-Rail Contact Theories and Their Implementation in Multibody Codes”. In: Jan. 2009. DOI: 10.1115/DETC2009-87655.

[38] *The GENSYS Homepage*.

[39] *Simpack Multibody System Simulation Software*. en.

[40] M. Sebès et al. “A fast-simplified wheel–rail contact model consistent with perfect plastic materials”. In: *Vehicle System Dynamics* 50.9 (Sept. 2012). Publisher: Taylor & Francis _eprint: https://doi.org/10.1080/00423114.2012.669483, pp. 1453–1471. DOI: 10.1080/00423114.2012.669483.

[41] L. Chevalier et al. “Taking into account plasticity in real time wheel-rail contact model”. In: *9th International Conference on Contact Mechanic and Wear of Rail/Wheel Systems*. Chengdu, China, 2012.

[42] N. Ohno and J. .-. Wang. “Kinematic hardening rules with critical state of dynamic recovery, part I: formulation and basic features for ratchetting behavior”. en. In: *International Journal of Plasticity* 9.3 (Jan. 1993), pp. 375–390. DOI: 10.1016/0749-6419(93)90042-O.

[43] R. Brommesson, M. Ekh, and M. Hörnqvist. “Correlation between crack length and load drop for low-cycle fatigue crack growth in Ti-6242”. en. In: *International Journal of Fatigue* 81 (Dec. 2015), pp. 1–9. DOI: 10.1016/j.ijfatigue.2015.07.006.

[44] J. Ahlström and B. Karlsson. “Fatigue behaviour of rail steel—a comparison between strain and stress controlled loading”. en. In: *Wear*. Contact Mechanics and Wear of Rail/Wheel Systems 258.7 (Mar. 2005), pp. 1187–1193. DOI: 10.1016/j.wear.2004.03.030.

[45] G. Johansson and M. Ekh. “On the modeling of large ratcheting strains with large time increments”. In: *Engineering Computations* 24.3 (Jan. 2007). Publisher: Emerald Group Publishing Limited, pp. 221–236. DOI: 10.1108/02644400710734945.

[46] S. Fouvry et al. “Wear analysis in fretting of hard coatings through a dissipated energy concept”. en. In: *Wear*. 11th International Conference on Wear of Materials 203-204 (Mar. 1997), pp. 393–403. DOI: 10.1016/S0043-1648(96)07436-4.

[47] A. Ekberg and E. Kabo. “Fatigue of railway wheels and rails under rolling contact and thermal loading—an overview”. en. In: *Wear*. Contact Mechanics and Wear of Rail/Wheel Systems 258.7 (Mar. 2005), pp. 1288–1300. DOI: 10.1016/j.wear.2004.03.039.

[48] A. R. S. Ponter, A. D. Hearle, and K. L. Johnson. “Application of the kinematical shakedown theorem to rolling and sliding point contacts”. en. In: *Journal of the Mechanics and Physics of Solids* 33.4 (Jan. 1985), pp. 339–362. DOI: 10.1016/0022-5096(85)90033-X.

[49] T. Telliskivi et al. “A tool and a method for FE analysis of wheel and rail interaction”. en. In: *Proceedings of the ANSYS 2000 Technical Conference, Pittsburg, US* (2000).

[50] Y. Jiang and H. Sehitoglu. “A model for rolling contact failure”. en. In: *Wear* 224.1 (Jan. 1999), pp. 38–49. DOI: 10.1016/S0043-1648(98)00311-1.

[51] M. C. Burstow. “Whole Life Rail Model Application and Development for RSSB – Continued Development of an RCF Damage Parameter”. en. In: *Rail Standards and Safety Board, London* 2 (2004), p. 74.

[52] J. L. Lumley. “The structure of inhomogeneous turbulent flows”. In: *Atmospheric Turbulence and Radio Wave Propagation* (1967). Publisher: Nauka, pp. 166–178.

[53] G. Berkooz, P. Holmes, and J. L. Lumley. “The Proper Orthogonal Decomposition in the Analysis of Turbulent Flows”. In: *Annual Review of Fluid Mechanics* 25.1 (1993). _eprint: https://doi.org/10.1146/annurev.fl.25.010193.002543, pp. 539–575. DOI: 10.1146/annurev.fl.25.010193.002543.

[54] A. Quarteroni, A. Manzoni, and F. Negri. *Reduced Basis Methods for Partial Differential Equations: An Introduction*. en. Google-Books-ID: e6FnCgAAQBAJ. Springer, Aug. 2015.

[55] F. Chinesta, R. Keunings, and A. Leygue. *The Proper Generalized Decomposition for Advanced Numerical Simulations*. en. SpringerBriefs in Applied Sciences and Technology. Cham: Springer International Publishing, 2014. DOI: 10.1007/978-3-319-02865-1.

[56] B. Bognet et al. “Advanced simulation of models defined in plate geometries: 3D solutions with 2D computational complexity”. en. In: *Computer Methods in Applied Mechanics and Engineering* 201-204 (Jan. 2012), pp. 1–12. DOI: 10.1016/j.cma.2011.08.025.

[57] E. Giner et al. “The Proper Generalized Decomposition (PGD) as a numerical procedure to solve 3D cracked plates in linear elastic fracture mechanics”. en. In: *International Journal of Solids and Structures* 50.10 (May 2013), pp. 1710–1720. DOI: 10.1016/j.ijsolstr.2013.01.039.

[58] J. F. Archard, W. Hirst, and T. E. Allibone. “The wear of metals under unlubricated conditions”. In: *Proceedings of the Royal Society of London. Series A. Mathematical and Physical Sciences* 236.1206 (Jan. 1997). Publisher: Royal Society, pp. 397–410. DOI: 10.1098/rspa.1956.0144.

Part II
Appended Papers A–C